# Energetic heterogeneity selects the folding nucleus of PDZ protein

Alexander Kluber[1,1], Cecilia Clementi[1,1]

**Abstract**

(250 word max) Energetic heterogeneity in structure-based models.

*Keywords:* structure-based model, Protein folding, folding nucleus

## 1. Introduction

Protein folding has come to serve as a pinacle problem for understanding biomolecular organization. One where simplified theories and models have been able to make important connections with experiment. Folding is possible on biological timescales because evolution has crafted the interactions in the folded structure to be in harmony when compared to the average misfolded alternative. The

Despite having the potential .

Single folding trajectories perform diffusion that is bias towards the native state.

The probability fluxes of folding trajectories are guided by the contours of the energy landscape.

The ensemble of folding routes can be imagined as following riverbeds in the free energy funneled landscapes. Upon close inspection these folding routes are braided amongst the microcorrugations .

Structure-based models have now become common practice in modeling of large biomolecules as they give access to longer timescale dynamics of biomolecules that fold to reasonably well-defined structures. Structure-based models are supported theoretically by the energy landscape theory of protein folding and in particular the principle of minimal frustration. The principle of minimal frustration states that heteropolymers searching for particle folded structure.

[1] [2] [3] [4]

Heuristically speaking .

Structure-based models started by using uniform contact strengths for all interactions (the homogeneous model). This would accurately describe cases where the average contact energies is representative of

[4]

Heterogeneous contact energies have been implemented in the literature by: Matysiak, Clementi Karanicolas, Brooks Cho, Wolynes

There are several simplified models of proteins that use funneling in their construction. The model of Karanicolas, Brooks incorporates energetic and backbone heterogeneity into .

The folding mechanisms of all $\beta$ proteins are robustly captured by structure-based models because heterogeneity in their native and non-natives contacts is self-averaging.

The quest for self-averaging properties.

A self-averaging properties.

Physical descriptors that characterize an esemble. For example, the radius of gyration and average collapse time of heteropolymer is a self-averaging property of sequences with the same hydrophobic content (average intrachain attraction).

Physical properties that can be captured.

Statistical physics seeks to make general statements about characterize p.

We want to characterize physical systems with simplified models.

The physica

because interactions.

Self-averaging

Considering all the contact energy distributions with similar characteristics (mean and variance), how do we show that ours leads to different physics?

Hypothesis: Arbitrary heterogeneity will lead to 1) broadening of the transition and 2) lower free energy barrier. [5] [6]

## 2. Results

We have found that structure-based models

Adding energetic heterogeneity to the structure-based model for PDZ shifts the center of the folding nucleus. The folding nucleus shifts from the beta1-beta2 hairpin in the homogeneous model to the C-terminus beta strands in the heterogeneous model.

We conclude that topology and heterogeneity are important for shaping the folding of PDZ.

Our procedure optimizes the model parameters in order to reproduce a given experimental observable. We chose to optimize our model using $\Delta\Delta G$'s from $\phi$-value analysis (as in Matysiak 2004), however the procedure used is general.

We claim that

Comparisons with the Wolynes group's frustratometer suggest.

When contact energies are uniform fluctuations in contact energy correlate with the growth of the folding nucleus. Contacts are collectively pulled into the nucleus.

Heterogeneity blurs the the nucleus. The folding nucleus of the .

If the prefactors are

## 3. Discussion

Proteins are minimally frustrated heteropolymers that can fold consistenly to well defined structures. Since their biological function requires interacting

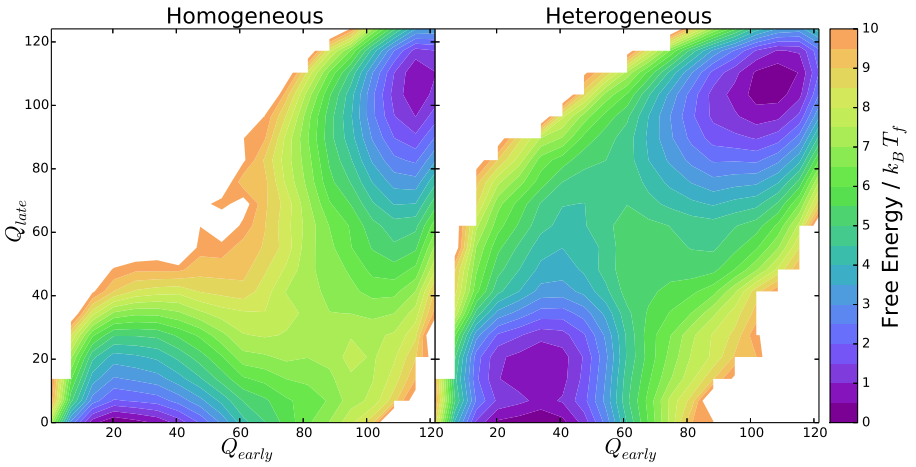


with other molecules, residual frustration occurs in their folded structures. It can be important to consider.

with respect to the function that have evolved to perform.

The model assumes the native state to be uniformly minimally frustrated. This leads to a natural preference for contacts that are close in sequence, such as helices, turns, and hairpins, due to their small entropic cost. However, real proteins may have localized frustration due to functional constraints during evolution (e.g. on binding faces).

The interplay of the backbone bias and existence of residual frustration can explain the three studied cases. In the cases of

PDZ and S6 have backbone and/or contact frustration in their folded structures in regions that are predicted to be too structured in the transition state in comparison with experiment. On the other hand SH3 has a minimally frustrated turn where it compares favorably with experiment.

How can we effectively capture local interactions that are not really minimally frustrated using structure-based models? - Optimize contact interactions - Optimize backbone interactions - Optimize both contact and backbone interactions - Use contact strengths derived from transferable potential - Use transferable backbone potential

Hypothesis: If I simultaneously optimize the contact and dihedral strengths will increased flexibility compensate for contact heterogeneity?

Raises question, is the nonlocal contact heterogeneity/frustration also important or the corrections only important for local interactions?

Sam Cho (2009) suggests that predictions will be more robust for proteins with a high nonlocal/local ratio. Our work indicates that the of .

Flexibility modulates the impact of heterogeneity/frustration.

However, real proteins are may have localized frustration in their folded states from functional considerations (Ferriero), which may be alleviated when they e.g. bind their intended partener.

The discrepancies of the homogeneous structure-based model with experiment observations can be understood when considering localized frustration explains.

This is why we observe repulsive native interactions.

have localized frustration in their native structures indicates that this hypothesis .

eal proteins

The homogeneous structure-based model assumes that protein interactions are uniformly unfrustrated throughout. However that may not be the case given that proteins have evolved their sequences to perform particular functions as well as fold. The folding nucleus 1 of PDZ includes residues frustration in the turn region.

Future work to design the beta hairpin of PDZ to favor nucleus 1.

Gianni 2007 has previous suggested that PDZ captures the essential features of nucleation-condensation folding mechanisms whereby the transition state ensemble is a diffuse nucleus center around the termini. Frustration.

All the parameters are not free in the sense that they are correlated. The Jacobian does not have full rank.

## 4. Materials and Methods

### *4.1. Structure-based model*

We use a "$C_\alpha$" structure-based model derived from [1], where the model Hamiltonian $H = H_{bonded} + H_{nonbonded}$ has a term that applies a local bias to the backbone $H_{bonded}$ and a term for the long-range interactions between residue beads $H_{nonbonded}$. The functional forms of these terms are,

$$H_{bonded} = \sum_{bonds} k_b(r_{ij} - r_{ij}^0)^2 + \sum_{angles} k_\theta(\theta_{ijk} - \theta_{ijk}^0)^2 + \tag{1}$$

$$\sum_{dihedrals} k_\phi[\cos(\phi_{ijkl} - \phi_{ijkl}^0) + \frac{1}{2}\cos(3(\phi_{ijkl} - \phi_{ijkl}^0))] \tag{2}$$

$$\tag{3}$$

$$H_{non-bonded} = \sum_{native} \epsilon_{ij} V_{ij}^{cont}(r_{ij}) + V_{ij}^{contex}(r_{ij}) \sum_{non-native} \epsilon_{ij}^{ex} \left(\frac{r_{ex}}{r_{ij}}\right)^{12} \tag{4}$$

Non-native contacts are given a purely repulsive potential of fixed strength $\epsilon_{ij}^{ex} = 1$ while native contacts are allowed to be attractive or repulsive with heterogeneous strengths. When two beads have an attractive interactions

Residue pairs that are not in contact in the native structure are given a purely repulsive

Contact maps were created using Shadow Map[7] via the SMOG webserver[8].

The starting point of our investigation is the homogeneous structure-based model derived from [**?** ] which places one bead per residue at the $C_\alpha$ positions of the backbone and creates attractive interactions between beads that are .

The energy scale of the model $\epsilon$ is constrained to its average value of the optimization.

places one bead per residues at the alpha-carbon positions of the backbones. Beads that are in contact in the folded structure are given attractive (or repulsive) native contact interactions. structure-based model is based off of

Our simplified model places one bead at the alpha-carbon of each residue. Bead have an excluded volume radius of 4angstroms. Residues that are in contact in the folded structure, "native contacts", are given an attractive gaussian interaction. The strengths of the native contacts is varied by the optimization algorithm in order to reproduce the .

A structure-based model is a simplified

$$H_{bonded} = \sum_{bonds} k_b(r_{ij} - r_{ij}^0)^2 + \sum_{angles} k_\theta(\theta_{ijk} - \theta_{ijk}^0)^2 + \tag{5}$$

$$\sum_{dihedrals} k_\phi[\cos(\phi_{ijkl} - \phi_{ijkl}^0) + \frac{1}{2}\cos(3(\phi_{ijkl} - \phi_{ijkl}^0))] \tag{6}$$

$$\tag{7}$$

The bonded constants used in this work are taken from Clementi et.al[1] and are (all in (kj/mol)): $k_b = 20000$, $k_\theta = 40$, $k_\phi = 1$.

The non-bonded Hamiltonian contains long-range interactions between beads.

$$H_{non-bonded} = \sum_{native} \epsilon_{ij} V_{ij}^{cont}(r_{ij}) + \sum_{non-native} \epsilon_{ij}^{ex} \left(\frac{r_{ex}}{r_{ij}}\right)^{12} \tag{8}$$

The Gaussian potential class takes the following forms,

$$V_{ij}^{G}(r_{ij}) = -e^{\frac{-(r_{ij}-r_{ij}^0)^2}{2\sigma_{ij}}} \tag{9}$$

$$V_{ij}^{Grep}(r_{ij}) = \frac{1}{2}\left[\tanh\left(-\left(\frac{r_{ij} - r_{ij}^0 - \ \sigma_{ij}}{\sigma_{ij}}\right)\right) + 1\right] \tag{10}$$

and requires adding an additional excluded volume to the corresponding pair in order to ensure that the contact potential is not perturbed at its equilibrium distance $r_{ij}^0$,

$$V_{ij}^{Gexc}(r_{ij}) = \left(\frac{r_{ex}^0}{r_{ij}}\right)^{12}\left(1 - \ e^{\frac{-(r_{ij}-r_{ij}^0)^2}{2\sigma_{ij}}}\right) \tag{11}$$

Homogeneous structure-based model developed by Clementi Implementation in gromacs using Shadow map, Gaussian contacts. SMOG. Noel, Lammert

*4.2. Parameter learning*

Parameter fitting algorithm developed by Matysiak, Clementi

$$\vec{f}^{sim}(\vec{\epsilon}) \approx \vec{f}^{sim}(\vec{\epsilon^{(0)}}) + \boldsymbol{J} \cdot \delta\vec{\epsilon} \tag{12}$$

Where (dropping the vector notation) $\delta\epsilon$ is some change in the model parameters and $\boldsymbol{J}$ encodes how that parameter change affects our simulation observable,

$$(\boldsymbol{J})_{ij} = \frac{\partial f_i^{sim}}{\partial \epsilon_j} \tag{13}$$

Setting equation 12 equal to the vector of experimental observables $\overline{f}$ and collecting the error $\delta f = f^{sim} - \overline{f}$ to the left-hand side yields,

$$-\delta f = \boldsymbol{J}\delta\epsilon \tag{14}$$

Which can be solved for the update to the model parameters $\delta\epsilon$ that will bring the simulated observables closer to the experimental values using standard tools for ill-posed problems (e.g. damped least-squares[9]; Singular Value Decomposition).[1] Overall this yields an iterative protocol for updating the model parameters which takes the form (on iteration $n$),

$$\epsilon^{(n+1)} = \epsilon^{(n)} + \delta\epsilon^{(n)} \tag{15}$$

The general procedure outlined above is iterated until satistfactory convergence. The specific form of the Jacobian matrix $\boldsymbol{J}$ depends on the specific observable being reproduced. Recall that the Jacobian is the partial derivative of the observable with respect to one of the model parameters,

$$(\boldsymbol{J})_{ij} = \frac{\partial f_i}{\partial \epsilon_j} \tag{16}$$

In most cases, the Jacobian $\boldsymbol{J}$ takes the simple form of a correlation function. For example, if $\vec{f}$ is any mechanical observable (i.e. anything computed solely from the coordinates), then,

$$\frac{\partial f_i}{\partial \epsilon_j} = -\beta \left[ \left\langle f_i \frac{\partial H}{\partial \epsilon_j} \right\rangle - \langle f_i \rangle \left\langle \frac{\partial H}{\partial \epsilon_j} \right\rangle \right] \tag{17}$$

This further simplifies for the linear Hamiltonian given by equation **??**,

$$\frac{\partial f_i}{\partial \epsilon_j} = -\beta \left[ \langle f_i V_j \rangle - \langle f_i \rangle \langle V_j \rangle \right] \tag{18}$$

[1] Note that even though there may be many more model parameters than observables, correlations between the corresponding potential energies mean that these parameters are not all truly independent. One way to quantify the lack of independence between parameters is by looking at the rank of the correlation matrix $c_{ij} = \langle V_i V_j \rangle - \langle V_i \rangle \langle V_j \rangle$, which has been found to have very low rank in this work (data available upon request).

In fact, the higher derivatives can also be obtained because they will always be joint cumulants of $f_i$ and the potential energies conjugate to the model parameters, $V_k$ (e.g. $\frac{\partial f_i}{\partial \epsilon_j \partial \epsilon_k}$ will be a second-order joint cumulant between $f_i$, $V_j$, and $V_k$). If desired a higher order method could be constructed using the second derivative in the Taylor expansion. However since the linear method convergences rather quickly and higher order methods are much more computationally demanding this direction hasn't been pursued. The Jacobian used to reproduce experimental $\Delta\Delta G$'s is slightly more involved and so is addressed in the next section.

In order to make the simulation and experimental energy scales comparable we put them in terms of $k_B T$ at their respective temperatures, then we multiply the experimental $\Delta\Delta G$'s by the following ratio $r = \frac{\overline{\Delta\Delta G_{sim}}}{\overline{\Delta\Delta G_{exp}}}$ in order to make the averages of the two equal ($r$ is only calculated from the initial homogeneous simulations and fixed thereafter). This can be understood as removing the systematic error and is justified because the coarse-grain model is defined on an arbitrary energy scale. Consequently we reproduce the true heterogeneity in the data, which is the deviation from the mean.

Modeling hydrophobic truncations as deletion of native contacts.

In simulation we model a mutation by perturbing the potential energy by $\Delta H_i$ for the $i$-th mutation,

$$H_i' = H + \Delta H_i \tag{19}$$

Naturally $\Delta H_i$ is calculated by subtracting some fraction of the contact energy from the mutated residue.

$$\Delta H_i = -\sum_j w_j^i \epsilon_j V_j \tag{20}$$

where the weight $w_j^i$ is calculated as the average fraction of heavy atom contacts lost when a mutation in the experimental structure. The purpose of the weight $w_j^i$ is to allow for different mutations at the same site. Mutations should perturb the energy proportional to the fraction of contacts they delete (e.g. L30V versus L30A). Then the free energy change resulting from the perturbation $\Delta H_i$ can be calculted using Zwanzig's relation [10],

$$\Delta G_i^X = -k_B T \ln \langle e^{-\beta \Delta H_i} \rangle_X \tag{21}$$

Where $X \in U, TS, N$ indicates the state we are perturbing, the unfolded (U), transition state (TS), or native state (N), respectively. The free energy profile along a reaction coordinate $Q$, e.g. the number of native contacts, is used to classify structures into states $U, TS, N$. The boundaries of the states are taken as $\frac{1}{3} k_B T$ from the corresponding minimum (for U,N states) or maximum (for TS). $Q$ has been shown to be an adequate reaction coordinate for folding in structure-based models [11].

Differentiating this expression with respect to our model parameter yields the difference of perturbed and unperturbed averages,

$$\frac{\partial \Delta G_i^X}{\partial \epsilon_j} = -\beta \left[ \left\langle \frac{\partial H_i'}{\partial \epsilon_j} \right\rangle_X' - \left\langle \frac{\partial H}{\partial \epsilon_j} \right\rangle_X \right] \tag{22}$$

where the primed average is taken with respect to Boltzman weights of $H_i'$, and can also be written as,

$$\frac{\partial \Delta G_i^X}{\partial \epsilon_j} = -\beta \left[ \frac{\left\langle e^{-\beta \Delta H_i} \frac{\partial (H + \Delta H_i)}{\partial \epsilon_j} \right\rangle_X}{\langle e^{-\beta \Delta H_i} \rangle_X} - \left\langle \frac{\partial H}{\partial \epsilon_j} \right\rangle_X \right] \tag{23}$$

Given our linear Hamiltonian from equation **??** and the perturbation in 20 this simplifies to,

$$\frac{\partial \Delta G_i^X}{\partial \epsilon_j} = -\beta \left[ \frac{\left\langle e^{-\beta \Delta H_i} (1 - w_j^i) V_j \right\rangle_X}{\langle e^{-\beta \Delta H_i} \rangle_X} - \langle V_j \rangle_X \right] \tag{24}$$

Finally, the Jacobian for the $\Delta\Delta G$'s is found from combining these expressions for the individual states as follows,

$$\frac{\partial \Delta\Delta G_i^{\ddagger}}{\partial \epsilon_j} = \frac{\partial \Delta G_i^{TS}}{\partial \epsilon_j} - \frac{\partial \Delta G_i^U}{\partial \epsilon_j} \tag{25}$$

$$\frac{\partial \Delta\Delta G_i^{\circ}}{\partial \epsilon_j} = \frac{\partial \Delta G_i^N}{\partial \epsilon_j} - \frac{\partial \Delta G_i^U}{\partial \epsilon_j} \tag{26}$$

## References


[1] C. Clementi, P. a. Jennings, J. N. Onuchic, How native-state topology affects the folding of dihydrofolate reductase and interleukin-1beta., Proc. Natl. Acad. Sci. 97 (11) (2000) 5871–6. doi:10.1073/pnas.100547897.
URL http://www.pubmedcentral.nih.gov/articlerender.fcgi?artid=18526&tool=pmcentrez&rend

[2] S. Matysiak, C. Clementi, Optimal combination of theory and experiment for the characterization of the protein folding landscape of S6: how far can a minimalist model go?, J. Mol. Biol. 343 (1) (2004) 235–48. doi:10.1016/j.jmb.2004.08.006.
URL http://www.ncbi.nlm.nih.gov/pubmed/15381433

[3] S. Matysiak, C. Clementi, Minimalist protein model as a diagnostic tool for misfolding and aggregation., J. Mol. Biol. 363 (1) (2006) 297–308. doi:10.1016/j.jmb.2006.07.088.
URL http://www.ncbi.nlm.nih.gov/pubmed/16959265

[4] S. Cho, Y. Levy, P. Wolynes, Quantitative criteria for native energetic heterogeneity influences in the prediction of protein folding kinetics, Proc. Natl. Acad. Sci.
URL http://www.pnas.org/content/106/2/434.short

[5] S. S. Plotkin, J. N. Onuchic, Structural and energetic heterogeneity in protein folding. I. Theory, J. Chem. Phys. 116 (12) (2002) 5263. doi:10.1063/1.1449866.
URL http://link.aip.org/link/JCPSA6/v116/i12/p5263/s1&Agg=doi

[6] B. Öztop, M. Ejtehadi, S. Plotkin, Protein Folding Rates Correlate with Heterogeneity of Folding Mechanism, Phys. Rev. Lett. 93 (20) (2004) 208105. doi:10.1103/PhysRevLett.93.208105.
URL http://link.aps.org/doi/10.1103/PhysRevLett.93.208105

[7] J. K. Noel, P. C. Whitford, J. N. Onuchic, The shadow map: a general contact definition for capturing the dynamics of biomolecular folding and function., J. Phys. Chem. B 116 (29) (2012) 8692–702. doi:10.1021/jp300852d.
URL http://www.pubmedcentral.nih.gov/articlerender.fcgi?artid=3406251&tool=pmcentrez&re

[8] J. K. Noel, P. C. Whitford, K. Y. Sanbonmatsu, J. N. Onuchic, SMOG@ctbp: simplified deployment of structure-based models in GROMACS., Nucleic Acids Res. 38 (Web Server issue) (2010) W657–61. doi:10.1093/nar/gkq498.
URL http://www.pubmedcentral.nih.gov/articlerender.fcgi?artid=2896113&tool=pmcentrez&re

[9] D. Marquardt, An algorithm for least-squares estimation of nonlinear parameters, J. Soc. Ind. Appl. ... 11 (2).
URL http://epubs.siam.org/doi/pdf/10.1137/0111030

[10] R. W. Zwanzig, High-Temperature Equation of State by a Perturbation Method. I. Nonpolar Gases, J. Chem. Phys. 22 (8) (1954) 1420. doi:10.1063/1.1740409.
URL http://link.aip.org/link/JCPSA6/v22/i8/p1420/s1&Agg=doi

[11] S. S. Cho, Y. Levy, P. G. Wolynes, P versus Q: structural reaction coordinates capture protein folding on smooth landscapes., Proc. Natl. Acad. Sci. 103 (3) (2006) 586–91. doi:10.1073/pnas.0509768103.
URL http://www.pubmedcentral.nih.gov/articlerender.fcgi?artid=1334664&tool=pmcentrez&re